International Journal of Aquatic Science
ISSN: 2008-8019
Vol 12, Issue 03, 2021

Automated Lung Nodule Candidate Detection Using An Iteratively Optimized Multi-Resolution 3D Depthwise Separable Cnns With Effective Training Initialization

Dr.V. Sumathi[1], Dr.N.Mahendiran[2]

[1]*Assistant Professor, Department of Computer Applications, Sri Ramakrishna College of Arts and Science, Coimbatore, India*
[2]*Assistant Professor, Department of Computer Science, Sri Ramakrishna College of Arts and Science, Coimbatore, India*

Abstract: An earlier detection and diagnosis of lung cancer requires a major task known as lung nodule candidate classification. To detect the lung nodule candidate, a Multi-Resolution 3-Dimensional Convolutional Neural Network and Knowledge Transfer (MR3DCNN-KT) model has been designed that can extract the contextual information between multiple samples of lung nodule image for increasing the detection accuracy. But, this model was not able to classify few types of nodules that may cause the false detection. Also, the training data preparation was high difficult due to the manual labeling that consumes more time and the label mistakes were introduced while using large scale datasets since 3D-CNN requires more number of samples. Hence this article proposes an Iteratively Optimized MR3DCNN-KT (IO-MR3DCNN-KT) model that establishes automated weak label initialization to classify the large scale lung nodule image datasets. This model is trained on dynamically updated training datasets in an iterative manner. A fast and automatic weak labeling scheme is applied to generate the initial training dataset. Nonetheless, the computational complexity of 3D-CNN structure is extremely high since it requires the significant number of computational resources. As a result, an IO-MR3D Depthwise Separable CNN and KT (IO-MR3D-DSCNN-KT) model is proposed that introduces the bottleneck-based 3D-DSCNN structure to reduce the computational complexity. This model can extract both spatial and temporal features using basic depthwise convolution and pointwise convolution, accordingly. Based on this model, the number of parameters used in the 3D-CNN structure is significantly reduced to automatically classify the lung nodule candidates. Finally, the experimental results show that the proposed model promises more accuracy and robustness compared to the MR3DCNN-KT model.

Keywords—Lung nodule candidate detection, MR3DCNN-KT, Bottleneck-based CNN, Weak label initialization, Depthwise convolution, pointwise convolution.

1. INTRODUCTION

Lung cancer is actually one of the leading causes of death and is stated to have poor levels of post-diagnosis survival in developing and undeveloped nations. Nevertheless, lung cancer may have a greater possibility of being recovered successfully if it is diagnosed immediately

instead of later. The prognosis of lung cancer is primarily based on the classification of the pulmonary or lung nodule. An essential means of successful medical treatment and avoidance of lung cancer is early lung nodule classification. The key recommendation for the classification of lung nodules will also be the Computed Tomography (CT) scans [1]. In fact, spatial analysis of CT images is a long-term method for radiological experts, since hundreds of samples are usually present on a specific scan and fewer than 100 voxels are available on a given nodule.

Modern Computer-Aided Detection (CAD) technologies were also designed to identify tiny nodules of the lung. This can be separated into CADe (Detection system) and CADs (Diagnostic system) [2-300]. CADe's primary objective is to identify Region-Of-Interests (ROIs) in the image, which may reveal different changes while the CADs's objective is to diagnose observed changes by category, volume, level and progress of epidemics. Two methods include the treatment of pulmonary nodules via CADs: raw nodule classification and nodule candidate detection [4]. The detection is important to the specific choice of lung nodules. The detection of a nodule candidate does also pose many difficulties such as radiological fluctuation and may lead some nodules to be invisible, while other non-nodules are termed as lung nodules that vary in scales and structure.

To avoid these limitations, an MRCNN-KT model was suggested in which standard 2D-CNN algorithm was enhanced as the new MR model via transferring its knowledge [5]. In this model, the knowledge was transferred from the source training processes and thus all the side-output branches in the model were considered for analyzing the features of various scales and resolutions from different depth layers in the CNN that classifies the lung nodule candidates. Moreover, objective and loss functions were developed as image-wise instead of pixel-wise representations. Further, samples creation and data augmentation were achieved for both training and testing the adapted classifier for identifying lung nodule candidates. Though the absolute lung nodule was often scattered on many samples, this 2D-CNN framework was restricted to extract the context features between multiple samples.

So, an MR3DCNN-KT model was introduced [6] to extract the context features between many samples. In this model, 3D convolutions were utilized for extracting the spatial and temporal features so that the context features encoded in the many neighboring samples were discovered. Based on this model, many channels of data were created from the input frames and the data from all the channels was combined for defining the final feature vector. Moreover, the outputs of high-level features were regularized and variety of outputs from CNN models was fused for increasing the detection accuracy. On the contrary, few types of nodules were not completely defined or classified which may lead to the false detection of lung nodule candidates. Although 3D-CNN for lung nodule candidate classification has high accuracy with an acceptable error for mistakenly labeled training networks, the training data preparation has high complexity since manual labeling was time-consuming and may introduce label errors in large scale datasets. Also, 3D-CNN needs more amount of samples than the 2D-CNN structure.

Therefore in this paper, an Iteratively Optimized MR3DCNN-KT (IO-MR3DCNN-KT) model is proposed that introduces automated weak label initialization for classifying the large scale datasets. This proposed IO-MR3DCNN-KT model is iteratively trained on dynamically updated training datasets. Particularly, the initial training dataset is generated based on the fast and automated weak labeling process that utilizes the maximal spatial overlap rate method. On the other hand, the 3D-CNN algorithm has high computational complexity due to its significant amount of computational resources. Hence, an IO-MR3D Depthwise Separable CNN and KT (IO-MR3D-DSCNN-KT) model is proposed for reducing the computational

complexity. In this model, a bottleneck-based 3D-DSCNN structure is introduced wherein the CT scan (lung nodule) image slices is split into spatial and temporal information. For learning spatial information, a fundamental depthwise convolution notion is applied to each lung image whereas the 3D pointwise convolution is applied for learning the temporal information i..e, the linear combination among sequential lung nodule image slices. This convolution is modified for reducing the parameter sizes of the 3D-CNN and efficiently achieving the lung nodule candidate detection. Thus, this model can reduce the computational complexity of 3D-CNN structure and learn the large scale lung nodule image datasets with labbeling weak labels automatically.

The rest of the article is prepared as follows: Section II presents the previous works accociated with the lung/pulmonary nodule detection using CNN. Section III explains the methodology of proposed model. Section IV demonstrates the experimental results and Section V concludes the article.

2. LITERATURE SURVEY

A multi-kernel based method [7] was proposed for selecting the features and learning the imbalanced data in lung nodule CAD. In this method, a multi-kernel feature selection was achieved on the basis of pairwise similarities from the feature level and a multi-kernel over-sampling for the imbalanced data learning. However, the computational complexity of this method was high.

A novel pulmonary nodule detection method [8] was proposed on the basis of Deep CNN (DCNN). Initially, a deconvolutional structure was introduced to Faster Region-based CNN (Faster R-CNN) for detecting lung nodule candidates on axial slices. After that, a 3D DCNN was proposed with the aid of dropout scheme for reducing the false positive in candidate detection. However, it does not consider the information between the small patches that were extracted in a large patch.

A novel approach was proposed using 3D CNN [9] to minimize the false positive in automated pulmonary nodule detection from volumetric CT scans. In this approach, more affluent spatial features were encoded and more representative features were extracted via their hierarchical structure trained with 3D samples. Also, an effective method was applied to encode the multilevel context information. Then, the final classification results were obtained via fusing the probability prediction results of these networks. But, the variances between the large variants of lung nodules and the restricted training dataset were not resolved.

A novel multi-view multi-scale CNN [10] was proposed for classifying the types of lung nodules from CT images. Initially, the spherical surface centred at nodules was approximated by icosahedra and the normalized sampling was captured for CT values on each circular view at a given highest radius. Then, intensity analysis was applied based on the sampled values for achieving estimated radius for each nodule. After that, the re-sampling was built followed by the high-frequency content measure analysis for choosing which views were richer in information. At last, the nodule captures at sorted scales and views were constructed for pre-training the view independent CNNs model and training the multi-view CNNs model with the maximum pooling. However, it cannot detect the tiny nodules and juxta-pleural nodules effectively.

A novel Multi-scale Gradual Integration CNN (MGI-CNN) algorithm [11] was suggested to learn the feature representations of multi-scale inputs using the gradual feature extraction scheme. In this algorithm, three major schemes were applied such as exploiting multi-scale inputs including various levels of context features, employing abstract information inherent in

various inputs scales with GI and training multi-stream feature fusion in an end-to-end way. Nonetheless, this algorithm has high False Positive (FP) rate.
A fusion algorithm [12] was introduced by fusing handcrafting features and the features trained at the output layers of a 3D CNN. Originally, various handcrafted features were extracted along with the intensity, geometric and texture features based on the gray-level co-occurrence matrix. Then, 3D CNNs were trained to extract the CNN features trained at the output layer. For each 3D CNN, the CNN features integrated with the handcrafted features were given as the input to the SVM fused with the sequential forward feature choice algorithm to elect the best feature subset and built the classifiers. But, this algorithm has less robustness.

3. PROPOSED METHODOLOGY

In this section, the proposed methodology for detecting the lung nodule candidates is explained in brief. At first, an IO-MR3DCNN-KT model is described using automated weak label initialization scheme. Then, an IO-MR3DSCNN-KT model is explained. The block diagram of the proposed lung nodule candidate detection models is shown in Figure 1.

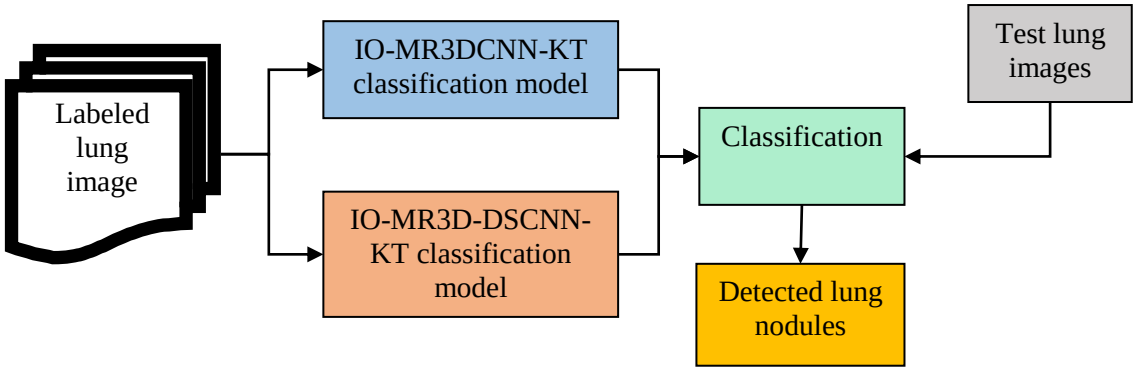

Figure 1. Block Diagram for Proposed Lung Nodule Detection Model

3.1 An Iterative Optimization of MR3DCNN-KT with Automated Weak Label Initialization for Lung Nodule Candidate Detection

Initially, the lung images are acquired from the Kaggle's Data Science Bowl 2017 (KDSB17) dataset. This dataset provides CT scan images of patients including their cancer status. But, it does not offer the positions or sizes of lung nodules. It comprises 2101 axial scans of patient chest cavities. Of the 2101, 1261 are belonging to the training set and 840 are belonging to the testing set. Each CT scan is labeled as "with cancer" if the related patient is diagnosed with cancer within 1 year of the scan; or else, labeled as "without cancer".

Pre-processing

Every scan is comprised of manifold 2D axial scans taken in sequence with pixel values in the range $(-1024,3071)$ respective to Hounsfield radiodensity units. The amount of slices, their thickness and scales are varied between each scan. Also, noise removal, spatial smoothing, temporal pre-whitening and linear registration to the lung template space are performed by the FSL FLIRT and FEAT commands. Once pre-processing is completed, the dictionary learning and sparse coding methods are used for functional lung networks restoration for each patient. The input for dictionary learning is a matrix $X \in \Re^{t \times n}$ with t rows and n columns containing normalized image pixels from n lung voxels of an individual

patient. The output has one learned dictionary D and a sparse coefficient matrix $a \in \Re^{m \times n}$ with respect to $X = D \times a + \varepsilon$ where ε denotes the error and m denotes the fixed dictionary size. After that, each row of the output coefficient matrix a is mapped to the lung volume space as a 3D spatial map of functional lung network.

IO-MR3DCNN-KT

This novel IO-MR3DCNN-KT is iteratively trained on dynamically updated training datasets. In particular, the initial training dataset is created by using a fast automated weak labeling mechanism that uses the maximal spatial overlap rate scheme for increasing the accuracy on detection with adequate training initialization. The classification labels are generated from KDSB17 dataset by using a clustering method based on the spatial overlap rate metric. Based on the classification labels, the large scale dataset of KDSB17 is used for detecting the lung nodule candidates.

According to the classification labels from KDSB17 dataset and the individual functional networks derived from KDSB17 dataset, the initial network labels are automatically and approximately allocated to each networks by computing the spatial overlap rate similarity matrix. The spatial overlap rate is computed as:

$$Overlap\ rate = \sum_{k=1}^{|V|} \frac{min(V_k, W_k)}{V_k + W_k / 2} \qquad (1)$$

In Eq. (1), V_k and W_k are the activation scores of voxel k in network volume maps V and W, accordingly. The empirical thresholding process is applied on the similarity matrix for ensuring the accuracy of the initial label assigned. For each individual network map, the label is allocated as classification labels whose spatial overlap rate is the maximum among all classification labels. If no similarity value is higher than 0.2, the respective network map is assigned the label 0 which will not be used for training. The IO-MR3DCNN-KT training process can iterate over l input 3D network maps for the maximum I iterations, initiating with the initial weak labels based on the spatial overlap rate. This spatial overlap rate-based classification achieves higher accuracy on detection while the CNN is able to correct the label for detection with increased accuracy. This label correction ability is adopted in this IO-MR3DCNN-KT model for increasing the previously allocated training labels during each iteration and so introducing the changes between labels detections after training and the labels before training. Once the iterative optimization is completed, a balance can be achieved by the IO-MR3DCNN-KT model while no significant changes happens; thus providing the optimized and well-trained MR3DCNN-KT model for functional lung nodule detection.

Algorithm: IO-MR3DCNN-KT Training Process

Input: KDSB17 dataset

Initialization:

1. Compute pairwise overlap rate between individual functional networks and functional labels $\rightarrow l \times n$ similarity matrix S^0;
2. Threshold overlap rate value in S less than 0.2 to be 0;

$\boldsymbol{for}(each\ individual\ network\ row\ S_i^0\ in\ S^0)$

$\boldsymbol{if}(S_i^0 = 0)$

$label_i = 0;$

$\boldsymbol{else}$

$label_i = argmax(S_i^0);$

$\{argmax(S_i^0) \in N | 1 \leq argmax(S_i^0) \leq n\};$

$\boldsymbol{end\ if}$

end for
Return $label^0$
//Deep Iterative Training: using no zero labeled individual functional networks and $label^0$ as initial training pairs
for$(i \in \{0,1,2,\dots,maxIter\})$
Train MR3DCNN-KT on
$[no\ zero\ labeled\ individual\ functional\ networks, label^i]$
$label^{i+1} = MR3DCNN - KT_{model}$ classify on all functional networks;
$label\_var = var(label^i, label^{i+1})$
if$(|label_{var}|/l < 0.4\%)$
Break
end if
end for
Return $MR3DCNN - KT_{model}$

Though it achieves better accuracy on detection of lung nodules, this 3D-CNN has high computational complexity due to the requirement of amount of parameters in 3D-CNN model. The 3D-CNN parameter is computed as:

$$P_{3D} = n \times c \times d(k \times k + 1) \quad (2)$$

In Eq. (2), n denotes the number of filters, k represents the spatial size of the convolutional kernel, d denotes the amount of temporal images and c indicates the amount of channels. When the input channels increase, the amount of parameter also increases. To tackle this problem, IO-MR3D-DSCNN-KT model is proposed which is explained below.

3.2 Effective Lung Nodule Candidate Detection Using Iteratively Optimized Multi-Resolution 3D-Depthwise Separable CNN and Knowledge Transfer

A novel IO-MR3D-DSCNN-KT model is proposed for effectively understanding the haptic force from lung images. For this purpose, the image is split into spatial and temporal information which are learnt independently and sequentially. In this model, the following processes are executed:

1. Spatial feature extraction: The 2D depthwise convolution is applied to each slice of the input image i.e., the process of learning the spatial information independent of the channel is applied to each slice.
2. Temporal feature extraction: The 3D pointwise convolution is applied for learning the linear combination among the channels among the channels of adjacent slices.

Initially, this 3D-DSCNN structure extracts the spatial information on the basis of the 2D depthwise convolution filters applied in the images. In this model, the shared weight parameters are used and the amount of these parameters is significantly reduced compared to the standard 3D-CNN model. Similarly, the 3D pointwise convolution filters are applied for extracting the temporal feature extraction. The concept of proposed IO-MR3D-DSCNN-KT model is shown in Figure 2.

The depthwise convolution filters $F_{depthwise} \in \Re^{k \times k}$ are trained separately based on their respective channels. This filter is fused with the pointwise convolution filter $F_{pointwise} \in \Re^{1 \times 1}$ for learning the correlation among the channels in the layer ends. While increasing the input channels, only the respective amount of filters is increased whereas the number of parameters used in the standard 3D-CNN model is not increased. Therefore, the sizes of the weight parameters are also derived as:

$$P_{3D} = n \times (c \times d + 1) + c \times (k \times k + 1) \quad (3)$$

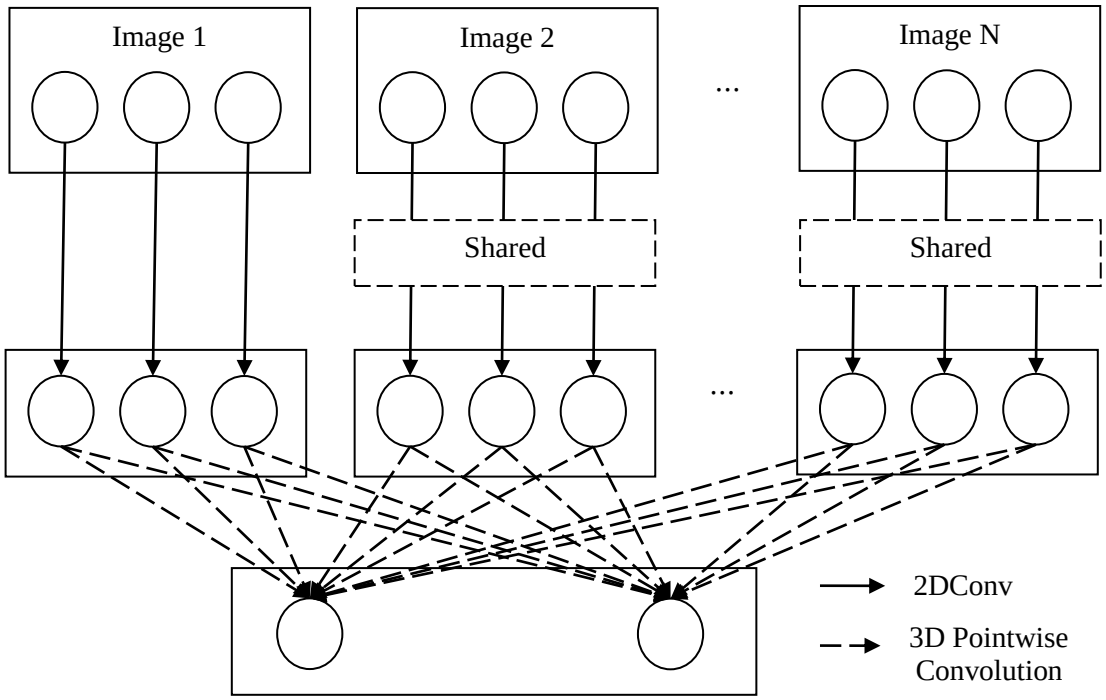

Figure 2. Concept of Proposed IO-MR3D-DSCNN-KT Model

This bottleneck 3D module is illustrated in Figure 3 for the inverted residual and basic linear block-based modules. The first layer of this module for increasing the number of channels is the pointwise convolution. The second layer is the depthwise convolutional filter with a $a \times a$ kernel and the 3D pointwise convolution is used in the last layer for learning the temporal information. Also, the depthwise convolutional filters are stacked successively for converting the temporal information to the salient information for detecting the lung nodules. The details of the network architecture of the IO-MR3D-DSCNN-KT model are provided in Table 1.

Table 1. Details of Network Structure of the IO-MR3D-DSCNN-KT Model

Layers	**Expand Channels**	**Output Channels**	**Spatial Stride**	**Kernel Depth**	**Depth Stride**
Conv2D 3 × 3	-	32	1	1	1
Bottleneck 3D 3 × 3 (a)	32	16	1	1	1
Bottleneck 3D 3 × 3 (a)	64	24	1	1	1
Bottleneck 3D 3 × 3 (a)	96	32	1	1	1
Bottleneck 3D 3 × 3 (b)	128	64	2	3	2
Bottleneck 3D 3 × 3 (b)	192	92	2	3	2
Bottleneck 3D 3 × 3 (b)	384	128	2	3	2
Bottleneck 3D 3 × 3 (b)	448	192	2	3	2
Conv2D 1 × 1	-	1280	2	2	2
Avg. Pool. 4 × 4	-	-	1	1	-
Fully Connected (FC) 1	-	1	-	-	-

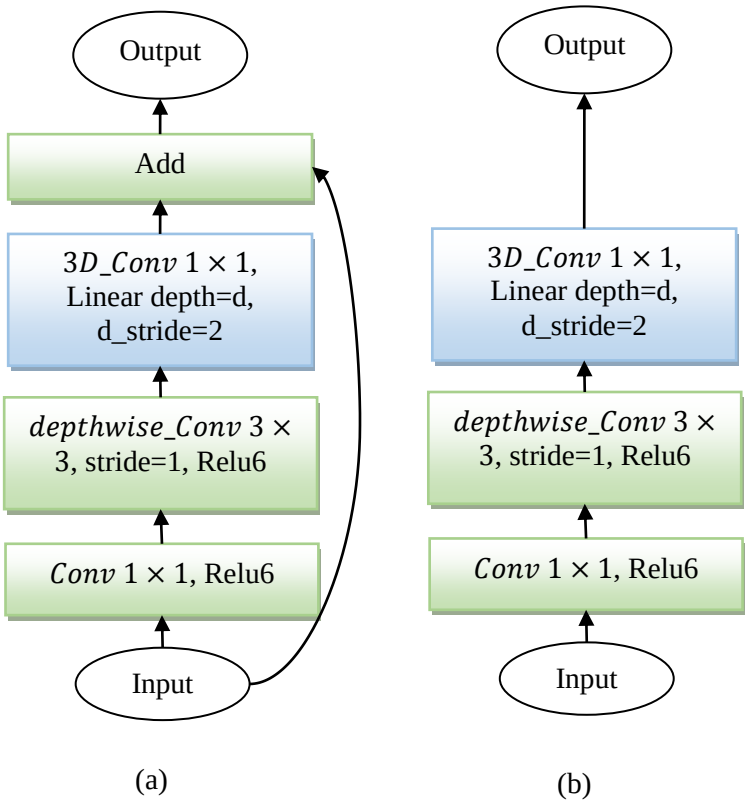

(a) (b)

Figure 3. IO-MR3D-DSCNN-KT Model based on (a) Inverted Residual Block and (b) Linear Block (Depthwise Convolutional Filter)

4. RESULTS AND DISCUSSION

In this section, the effectiveness of IO-MR3DCNN-KT and IO-MR3D-DSCNN-KT models is evaluated as well as compared with the MR3DCNN-KT model using MATLAB 2018a. Given a KDSB17 dataset, 1261 data are used for training and 840 data are u sed for testing process. This comparative analysis is performed in terms of precision, recall, f-measure, accuracy, error rate and separability. Figure 4 shows the experimental outcomes of the IO-MR3DCNN-KT and existing MR3DCNN-KT models for lung nodule detection. Similarly, Figure 5 illustrates the experimental outcomes of the IO-MR3D-DSCNN-KT and IO-MR3DCNN-KT models for detecting the lung nodules.

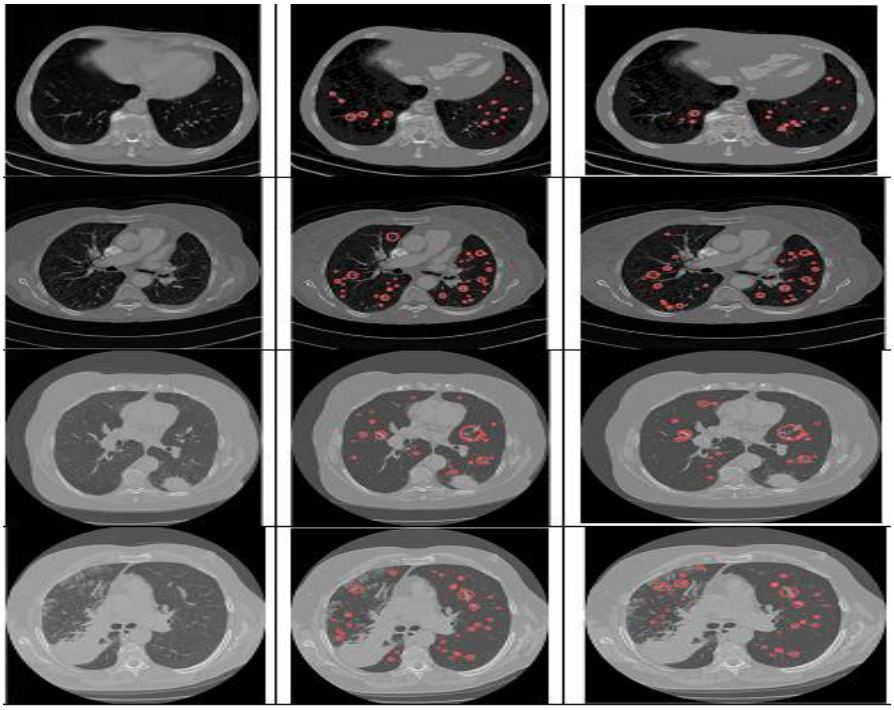

(a) (b) (c)

Figure 4. Results of Lung Nodule Candidate Detection Models: (a) Input Image (b) Detected Nodules using MR3DCNN–KT (c) Detected Nodules using IO-MR3DCNN–KT

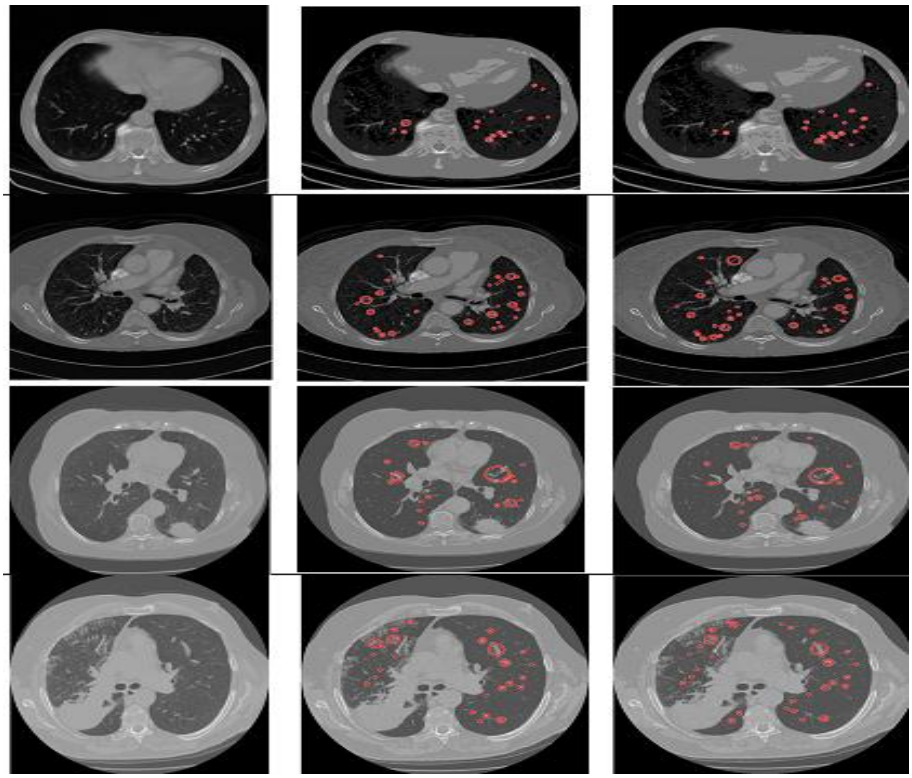

(a) (b) (c)

Figure 5. Results of Lung Nodule Candidate Detection Models: (a) Input Image (b) Detected Nodules using IO-MR3DCNN–KT (c) Detected Nodules using IO-MR3D-DSCNN–KT

4.1 Precision

It is a measure computed based on the detection of lung nodules at True Positive (TP) and False Positive (FP) rates.

$$Precision = \frac{TP}{TP+FP} \quad (4)$$

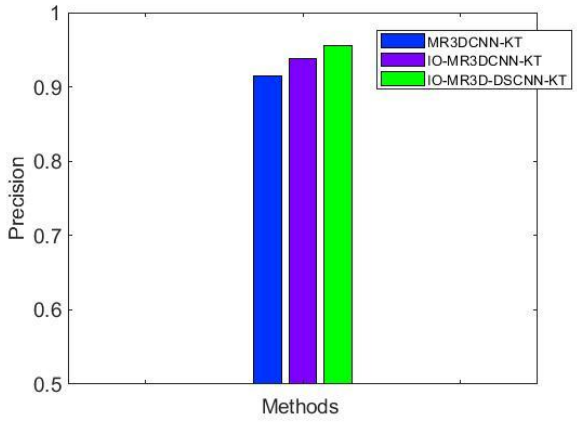

Figure 6. Comparison of Precision

In Figure 6, the precision values for IO-MR3D-DSCNN-KT, IO-MR3DCNN-KT and MR3DCNN-KT models are illustrated. Through this analysis, it is recognized that the precision of IO-MR3D-DSCNN-KT is 1.84% higher than the IO-MR3DCNN-KT and 4.52% higher than MR3DCNN-KT models.

4.2 Recall

It is calculated on the basis of detecting the lung nodules at TP and False Negative (FN) rates.

$$Recall = \frac{TP}{TP+FN} \quad (5)$$

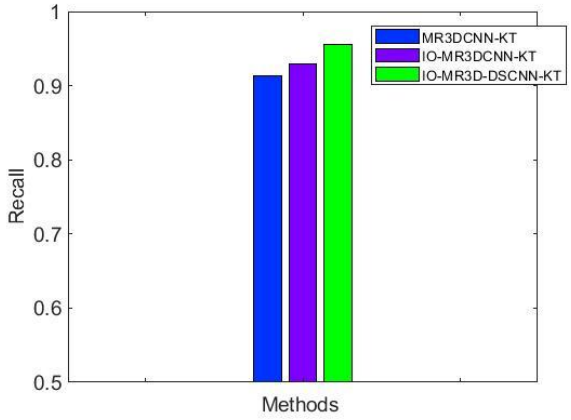

Figure 7. Comparison of Recall

Figure 7 shows the recall values for IO-MR3D-DSCNN-KT, IO-MR3DCNN-KT and MR3DCNN-KT models. By using this analysis, it is noticed that the recall of IO-MR3D-DSCNN-KT is 2.68% higher than the IO-MR3DCNN-KT and 4.53% higher than MR3DCNN-KT models.

4.3 F-measure

It is the harmonic mean of both precision and recall.

$$F - measure = \frac{2 \cdot Precision \cdot Recall}{Precision + Recall} \quad (6)$$

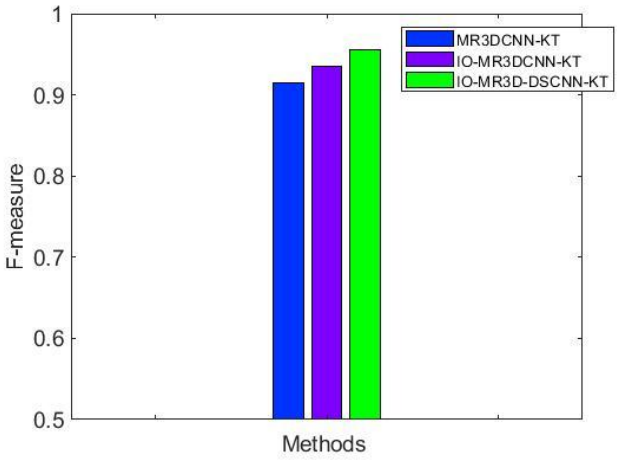

Figure 8. Comparison of F-measure

In Figure 8, the f-measure values for IO-MR3D-DSCNN-KT, IO-MR3DCNN-KT and MR3DCNN-KT models are illustrated. From this analysis, it is observed that the f-measure of IO-MR3D-DSCNN-KT is 2.18% higher than the IO-MR3DCNN-KT and 4.53% higher than MR3DCNN-KT models.

4.4 Accuracy

It is the ratio of accurate lung nodule detection over the total amount of instances evaluated.

$$Accuracy = \frac{TP+True\ Negative\ (TN)}{TP+TN+FP+FN} \qquad (7)$$

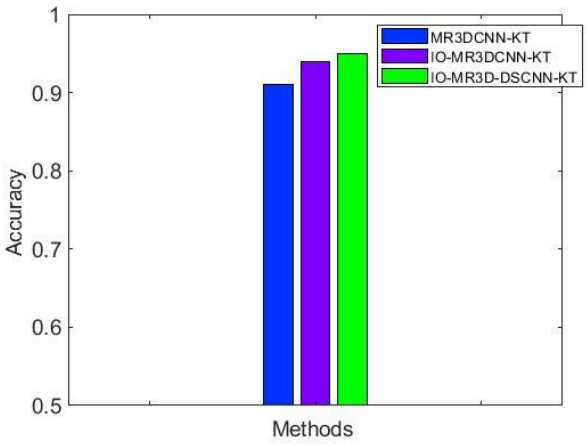

Figure 9. Comparison of Accuracy

Figure 9 shows the accuracy values for IO-MR3D-DSCNN-KT, IO-MR3DCNN-KT and MR3DCNN-KT models. From this analysis, it is addressed that the accuracy of IO-MR3D-DSCNN-KT is 1.06% higher than the IO-MR3DCNN-KT and 4.4% higher than MR3DCNN-KT models.

4.5 Error Rate

It is measured as:

$$Error\ rate = \frac{FP+FN}{TP+TN+FP+FN} \qquad (8)$$

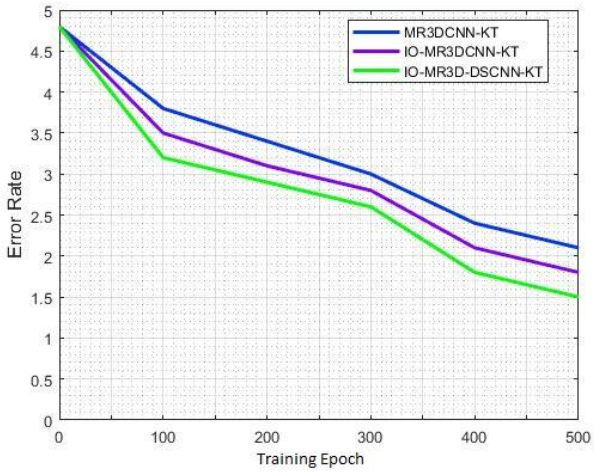

Figure 10. Comparison of Error Rate

In Figure 10, the error rate values for IO-MR3D-DSCNN-KT, IO-MR3DCNN-KT and MR3DCNN-KT models are shown. In this graph, x-axis denotes the number of training epochs and y-axis denotes the error rate values. From this analysis, it is observed that the error rate of IO-MR3D-DSCNN-KT is 27.12% less than the IO-MR3DCNN-KT and 28.57% less than MR3DCNN-KT models while considering 500 training epochs.

4.6 Separability

It is the separability of the data representation in different layers and computed as follows:

$$Separability = \frac{\sum_i \left(\overline{x^l} - \bar{x}\right)^2}{\sum_i {}^1/_{n^i - 1} \sum_j \left(x_j^i - \overline{x^l}\right)^2} \qquad (9)$$

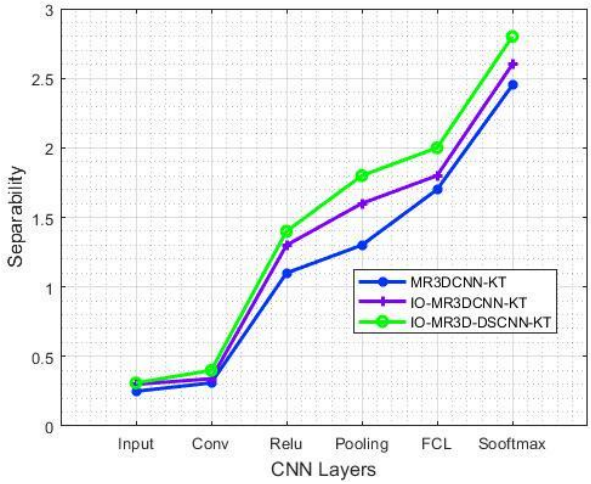

Figure 11. Comparison of Separability

Figure 11 shows the separability values of IO-MR3D-DSCNN-KT, IO-MR3DCNN-KT and MR3DCNN-KT models for different layers in CNN architecture. In this graph, x-axis denotes the types of CNN layers and y-axis denotes the separability values. In case of softmax layer, the separability of IO-MR3D-DSCNN-KT is 7.69% higher than IO-MR3DCNN-KT and 14.29% higher than MR3DCNN-KT models.

5. CONCLUSION

In this article, an IO-MR3DCNN-KT model is proposed for achieving training initialization using automated weak labeling process. This model is mainly applied for generating the initial training dataset which is trained in an iterative manner. But, this model has high computational complexity. Thus, an IO-MR3D-DSCNN-KT model is proposed that comprises the bottleneck-based 3D-DSCNN architecture for minimizing the computational complexity of 3D-CNN structure. In this model, both spatial and temporal features are extracted via fundamental depthwise convolution and pointwise convolution, correspondingly, for classifying the lung nodule candidates with reduced number of parameters in the 3D-CNN structure. Finally, the experimental results proved that the IO-MR3D-DSCNN-KT model achieves better performance in terms of precision, recall, f-measure, accuracy, error rate and separability than the both IO-MR3DCNN-KT and MR3DCNN-KT models.

6. REFERENCES

[1] Bach, P. B., Mirkin, J. N., Oliver, T. K., Azzoli, C. G., Berry, D. A., Brawley, O. W., ... & Sabichi, A. L. (2012). Benefits and harms of CT screening for lung cancer: a systematic review. *Jama*, *307*(22), 2418-2429.

[2] Messay, T., Hardie, R. C., & Rogers, S. K. (2010). A new computationally efficient CAD system for pulmonary nodule detection in CT imagery. *Medical image analysis*, *14*(3), 390-406.

[3] Javaid, M., Javid, M., Rehman, M. Z. U., & Shah, S. I. A. (2016). A novel approach to CAD system for the detection of lung nodules in CT images. *Computer methods and programs in biomedicine*, *135*, 125-139.

[4] Setio, A. A. A., Traverso, A., De Bel, T., Berens, M. S., van den Bogaard, C., Cerello, P., ... & van der Gugten, R. (2017). Validation, comparison, and combination of algorithms for automatic detection of pulmonary nodules in computed tomography images: the LUNA16 challenge. *Medical image analysis*, *42*, 1-13.

[5] Zuo, W., Zhou, F., Li, Z., & Wang, L. (2019). Multi-resolution CNN and knowledge transfer for candidate classification in lung nodule detection. *IEEE Access*, *7*, 32510-32521.

[6] P. B. Pankajavalli, G. S. Karthick and R. Sakthivel, "An Efficient Machine Learning Framework for Stress Prediction via Sensor Integrated Keyboard Data," in IEEE Access, vol. 9, pp. 95023-95035, 2021, doi: 10.1109/ACCESS.2021.3094334.

[7] Cao, P., Liu, X., Yang, J., Zhao, D., Li, W., Huang, M., & Zaiane, O. (2017). A multi-kernel based framework for heterogeneous feature selection and over-sampling for computer-aided detection of pulmonary nodules. *Pattern Recognition*, *64*, 327-346.

[8] G. S. Karthick and P. B. Pankajavalli, "Ambient intelligence for patient-centric healthcare delivery: Technologies framework and applications" in Design Frameworks for Wireless Networks, Singapore:Springer, pp. 223-254, Oct. 2020.

[9] Dou, Q., Chen, H., Yu, L., Qin, J., & Heng, P. A. (2017). Multilevel contextual 3-D CNNs for false positive reduction in pulmonary nodule detection. *IEEE Transactions on Biomedical Engineering*, *64*(7), 1558-1567.

[10] Liu, X., Hou, F., Qin, H., & Hao, A. (2017). Multi-view multi-scale CNNs for lung nodule type classification from CT images. *Pattern Recognition*, *77*, 262-275.

[11] Kim, B. C., Yoon, J. S., Choi, J. S., & Suk, H. I. (2019). Multi-scale gradual integration CNN for false positive reduction in pulmonary nodule detection. *Neural Networks*, *115*, 1-10.
[12] Li, S., Xu, P., Li, B., Chen, L., Zhou, Z., Hao, H., ... & Jiang, S. (2019). Predicting lung nodule malignancies by combining deep convolutional neural network and handcrafted features. *Physics in Medicine & Biology*, *64*(17), 175012.